Since January 2020 Elsevier has created a COVID-19 resource centre with free information in English and Mandarin on the novel coronavirus COVID-19. The COVID-19 resource centre is hosted on Elsevier Connect, the company's public news and information website.

Available online at www.sciencedirect.com
SCIENCE DIRECT®
Analytical Biochemistry 345 (2005) 214–226
ANALYTICAL BIOCHEMISTRY
www.elsevier.com/locate/yabio

A surface plasmon resonance-based assay for small molecule inhibitors of human cyclophilin A

Martin A. Wear [a], Alan Patterson [a], Kirk Malone [b], Colin Dunsmore [b], Nicholas J. Turner [b], Malcolm D. Walkinshaw [a,*]

[a] *Institute of Structural and Molecular Biology, School of Biological Sciences, University of Edinburgh, Edinburgh EH9 3JR, UK*
[b] *School of Chemistry, University of Edinburgh, Edinburgh EH9 3JR, UK*

Received 6 May 2005
Available online 12 July 2005

Abstract

A simple protocol for generating a highly stable and active surface plasmon resonance (SPR) sensor surface of recombinant human hexahistidine cyclophilin A (His-CypA) is described. The sensor surface was sensitive and stable enough to allow, for the first time, the screening and ranking of several novel small-molecule (M_r ~250–500 Da) ligands in a competition binding assay with cyclosporin A (CsA). It also allowed us to accurately determine the kinetic rate constants for the interaction between His-CypA and CsA. His-CypA was first captured on a Ni^{2+}–nitrilotriacetic acid (NTA) sensor chip and was then briefly covalently stabilized, coupling via primary amines. The significant baseline drift observed due to dissociation of weakly bound His-CypA from the Ni^{2+}–NTA moiety was eliminated, resulting in a surface that was stable for at least 36 h. In addition, immobilized protein activity levels were high, typically between 85 and 95%, assayed by the interaction between His-CypA and CsA. The mean equilibrium dissociation constant for CsA (K_{dCsA}) binding to the immobilized His-CypA was 23 ± 6 nM, with on and off rates of 0.53 ± 0.1 μM^{-1} s^{-1} and 1.2 ± 0.1 ($\times 10^{-2}$) s^{-1}, respectively. These values agree well with the values for the corresponding binding constants determined from steady-state and kinetic fluorescence titrations in solution.

Keywords: Surface plasmon resonance; Cyclophilin A; Cyclosporin A; Competition binding assay

Surface plasmon resonance (SPR)[1] is now a technique exploited regularly in the determination of equilibrium binding and kinetic rate constants of biomolecular interactions [1–4]. It is also increasingly useful in drug discovery/hit validation studies with small molecules [4–11]. A prerequisite for measuring the binding constants of an interaction by SPR is that the surface-immobilized molecule must be both stably attached and highly active. Most immobilization procedures are reliant on direct covalent linkage of a purified protein to chemically activated sensor surfaces. Such procedures generate stable surfaces. However, a significant proportion of proteins are not compatible with either the solution conditions or the surface chemistry used. As a result, many biomolecules have very low activity, or often become completely inactive, on immobilization. Over and above the loss of activity due to modification of critical residues involved in binding sites, the essentially random orientation resulting from

* Corresponding author.
E-mail address: m.walkinshaw@ed.ac.uk (M.D. Walkinshaw).

[1] *Abbreviations used:* SPR, surface plasmon resonance; NTA, nitrilotriacetic acid; His-CypA, hexahistidine cyclophilin A; CypA, cyclophilin A; PPIase, peptidyl-prolyl isomerase; CsA, cyclosporin A; SA, streptavidin; PCR, polymerase chain reaction; IPTG, isopropylthiogalactoside; DTT, dithiothreitol; EDTA, ethylenediamine tetraacetic acid; PMSF, phenylmethanesulfonyl fluoride; EDC, 1-ethyl-3-(3-diaminopropyl) carbodiimide hydrochloride; NHS, *N*-hydroxysuccinimide; RU, response units; DMSO, dimethyl sulfoxide; ITC, isothermal titration calorimetry; BSA, bovine serum albumin.

0003-2697/$ - see front matter © 2005 Elsevier Inc. All rights reserved.
doi:10.1016/j.ab.2005.06.037

covalent coupling leads to subpopulations of immobilized molecules that are incorrectly oriented for binding. There are a number of capture methods available (e.g., antibodies, biotinylation, oligohistidine tags) that can be used as alternatives to direct covalent coupling. However, the sensor surface often has a relatively low binding capacity and/or exhibits significant baseline drift due to the relatively weakly bound captured molecule dissociating from the surface. For example, single hexahistidine-tagged proteins captured on Ni^{2+}–nitrilotriacetic acid (NTA) sensor surfaces have K_d values in the low micromolar range [12]. Such leaching makes it difficult to assess binding kinetics accurately.

Here, we describe the generation of a highly stable and active sensor surface of an N-terminally tagged hexahistidine cyclophilin A (His-CypA), which has enabled a series of ligand binding studies with nonpeptide small molecules to be performed. The cyclophilins [13] have emerged recently as a potential drug target for a several diseases, including HIV and malaria infection [14,15]. The SPR-based binding assay described here provides the basis of a screen for novel small-molecule cyclophilin inhibitors of potential therapeutic interest. The in vivo role of human cyclophilin A (CypA) is poorly understood, but its ability to enhance the rate of folding (or unfolding) of proteins via its peptidyl-prolyl isomerase (PPIase) activity is likely to be important, particularly when the cell is stressed [13,16]. CypA was isolated as a complex with the immunosuppressive cyclic undecapeptide cyclosporin A (CsA) [17], which is used as a therapy for preventing organ rejection following transplants. CsA acts by complex formation with cytosolic CypA, followed by binding and inhibition of the phosphatase calcineurin, blocking the signal transduction pathway for immunostimulation [18]. Previous work has identified many cyclosporin derivatives as CypA inhibitors [19–25], but there are very few published examples that characterize nonpeptide inhibitor binding [26,27].

The development of an SPR-based assay for screening small-molecule ligands requires a stable and sensitive CypA sensor surface. Human CypA is not readily amenable to direct covalent immobilization on a CM5 sensor, or on a streptavidin (SA) sensor, using standard coupling chemistries. In our hands, these coupling protocols generated surfaces with very low levels of protein activity, typically only approximately 5%. Surfaces with such low levels of activity are neither active nor sensitive enough to facilitate the detection of small molecules. Although interactions between CypA, directly coupled to the sensor surface, and protein binding partners analyzed by SPR have been published [28–30], the activity of immobilized protein and the sensitivity of the sensor required to detect binding of these much larger molecules are significantly less than those needed to detect small-molecule ligands. In contrast, when His-CypA was first captured and oriented via its N-terminal hexahistidine tag on an NTA sensor surface and then was briefly covalently stabilized, using standard chemistries to activate the surface and couple via primary amines, the baseline drift was completely eliminated and the surface activity levels typically were in excess of 85%. These sensor surfaces allowed us, for the first time, to assess and rank the equilibrium dissociation constants (K_d) for several new small-molecule (~300–500 Da) inhibitors of CypA.

Materials and methods

Materials

All chemicals used were of the highest grade available commercially.

Plasmid construction

The plasmids for expression of recombinant human CypA were created by polymerase chain reaction (PCR) using a whole tissue human lung cDNA library (Stratagene) as a template, with 5′-CCATGGTCAA CCCCACCGTGTTC-3′ as the forward primer and 5′-GGATCCTTATTCGAGTTGTCCACAGTC-3′ as the reverse primer. The resulting PCR product was verified by sequencing in both directions, using ABI PRISM BigDye v3 Terminator Cycle Sequencing Ready Reaction Kit and an ABI PRISM 310 genetic analyzer (Applied Biosystems). For generation of the untagged CypA expression vector, *pSW3-001*, the PCR product was digested with *Nco*I and *Bam*HI (New England BioLabs) and then ligated into a pET-5a vector (Novagen) digested with *Nco*I and *Bam*HI. For generation of the N-terminal His-CypA expression vector, *pSW3-002*, the *Nco*I and *Bam*HI digested PCR product was ligated into a pET-15b vector (Novagen) similarly digested. Correct insertion of the coding region of CypA was verified by restriction digest and by sequencing the entire coding region in both directions.

Protein expression and purification

All purification was performed on ÅKTA Prime (Pharmacia) equipment at 4 °C.

His-CypA purification

Recombinant human His-CypA was expressed and purified to homogeneity from BL21 (DE3) *Escherichia coli* (Novagen). LB media containing carbenicillin (100 μg ml^{-1}) were grown shaking (260 rpm) at 37 °C until the A_{600nm} was approximately 0.6. Overexpression of His-CypA was induced by the addition of isopropyl-thiogalactoside (IPTG) to 1 mM and growth for a further 3 h at 37 °C. Lysis and purification, on NTA agarose resin (Qiagen), was performed according to

standard protocols. Fractions containing His-CypA were pooled, concentrated to $\leqslant$1 ml, filtered through a 0.2-μm filter, and loaded onto a Sephacryl 200 HR (Pharmacia) gel filtration column ($V_t \sim 1.6 \times 60$ cm) preequilibrated in 25 mM Tris (pH 7.5), 100 mM NaCl, 0.5 mM dithiothreitol (DTT), 0.5 mM ethylenediamine tetraacetic acid (EDTA), and 1 mM NaN_3. His-CypA was more than 95% pure as judged by SDS–PAGE.

Untagged CypA purification

Recombinant human CypA was expressed and purified to homogeneity from BL21 Star (DE3) *E. coli* (Invitrogen). 2 × TY liquid media containing carbenicillin (100 μg ml^{-1}) was grown at 37 °C until the A_{600nm} was approximately 0.6. Overexpression of CypA was induced by the addition of IPTG to 1 mM and growth for a further 3 h at 37 °C. Cells were harvested by centrifugation (3000*g* for 15 min) and washed once in 100 ml of lysis buffer (50 mM Hepes [pH 7.5], 1 mM DTT, 2.5 mM EDTA, 1 mM NaN_3). The cell pellet was resuspended at 10% weight per volume in ice-cold lysis buffer plus excess protease inhibitor cocktail (Sigma) and sonicated on ice for 6 × 30-s bursts with 30 s cooling in between. The cell lysate was subjected to centrifugation at 50,000*g* for 1 h at 4 °C. The high-speed supernatant was dialyzed exhaustively overnight against 50 mM Hepes (pH 6.8), 1 mM DTT, 2.5 mM EDTA, 1 mM NaN_3, 100 μM phenylmethanesulfonyl fluoride (PMSF), and 100 μM benzamidine; filtered through a 0.2-μm filter; and applied to an SP Sepharose (Pharmacia) column ($V_t \sim 50$ ml, 2.6×10 cm) preequilibrated in the same buffer. Proteins were eluted with a 0- to 400-mM NaCl gradient in the same buffer over 200 ml and were analyzed by SDS–PAGE. Fractions containing CypA, eluting between 130 and 160 mM NaCl, were pooled, concentrated to approximately 1 ml, filtered through a 0.2-μm filter, and loaded onto a Sephacryl 200 HR gel filtration column ($V_t \sim 120$ ml, 1.6×60 cm) preequilibrated in 25 mM Tris (pH 7.5), 100 mM NaCl, 0.5 mM DTT, 0.5 mM EDTA, and 1 mM NaN_3. CypA was more than 95% pure as judged by SDS–PAGE.

SPR equipment and reagents

SPR measurements were performed on a Biacore 3000 instrument kindly provided on loan from Biacore. Research-grade CM5, SA, and NTA sensors were used. The reagents 1-ethyl-3-(3-diaminopropyl) carbodiimide hydrochloride (EDC) and *N*-hydroxysuccinimide (NHS) were purchased from Biacore and used according to recommended protocols.

Immobilization and covalent stabilization of His-CypA

Pure His-CypA was immobilized on an NTA sensor chip. The sensor was primed and loaded with Ni^{2+} according to Biacore's recommended protocols. His-CypA in 10 mM Hepes (pH 7.4), 150 mM NaCl, 0.005% surfactant P20, and 2% ethanol, at concentrations between 200 nM and 1 μM, was passed over the sensor surface at a flow rate of 5 μl min^{-1}. Following saturation of the response units (RU) signal, a 30-s injection (at 15 μl min^{-1}) of a mixture of NHS (115 mg ml^{-1}) and EDC (750 mg ml^{-1}), followed immediately followed by a 30-s injection (at 15 μl min^{-1}) of 1 M ethanolamine (pH 8.5), was performed. The final amount of His-CypA covalently immobilized on the surface was typically between 850 and 1600 RU.

Covalent immobilization of untagged CypA

Pure CypA was immobilized on a CM5 sensor chip. HBS-EP2 buffer (10 mM Hepes [pH 7.4], 150 mM NaCl, 3 mM EDTA, 0.005% surfactant P20, 2% ethanol) was used as running buffer. Activation of the sensor chip surface was performed with a mixture of NHS (115 mg ml^{-1}) and EDC (750 mg ml^{-1}) for 7 min at 5 μl min^{-1}. CypA was diluted with 10 mM acetate buffer (pH 4.9) to a final concentration of between 10 and 50 μg ml^{-1}. The amount of CypA immobilized on the activated surface was controlled by altering the contact time of the protein solution and was between approximately 1000 and 5000 RU. After the immobilization of the protein, a 7-min injection (at 5 μl min^{-1}) of 1 M ethanolamine (pH 8.5) was used to quench excess active succinimide ester groups.

Immobilization of biotinylated CypA

Pure CypA was biotinylated using the EZ Link NHS-LC-Biotin kit (Pierce) according to recommended protocols. The protein was then immobilized on an SA sensor chip, according to Biacore's recommended protocols, in HBS-EP2 buffer at 5 μl min^{-1}. The final amount of Bio-CypA covalently immobilized on the SA surface was 1811 RU.

SPR binding experiments with CsA

SPR binding experiments with CsA were performed in HBS-EP2 buffer as the running buffer. The flow rate was 50 μl min^{-1} in all experiments. The sensor surface was regenerated between experiments by dissociating any formed complex in HBS-EP2 buffer for 30 min, followed by a further 30-min stabilization period. CypA is not amenable to more stringent and rapid regeneration conditions (data not shown). Furthermore, CsA is a hydrophobic molecule with limited solubility in aqueous solutions and has a tendency to adhere to tubing and tips at concentrations greater than 1.2 μM. Ethanol (2%) was used in experimental running buffers to help alleviate solubility problems. Ethanol was used in

preference to dimethyl sulfoxide (DMSO) because this binds weakly to CypA [31]. The 60-min total regeneration time between experiments helped to eliminate any carryover of CsA [32]. A concentration series of CsA ranging from 0.5 nM to 1.2 μM was typically run in these experiments. The binding curves were analyzed for a one-to-one Langmuir binding model provided by with the Biacore 3000 instrument software.

SPR competition binding experiments

SPR competition experiments were performed in HBS-EP2 buffer. A fixed concentration (25 nM) of CsA in the presence of increasing concentrations of the respective small molecule was passed over a covalently stabilized His-CypA sensor surface for 5 min at 50 μl min^{-1}. The sensor surface was regenerated between experiments by dissociating any formed complex in HBS-EP2 buffer for 30 min, followed by a further 30-min stabilization period. The binding curves were analyzed using the heterogeneous analyte competition model (i.e., CsA and the small molecule compete for the same single binding site on CypA) supplied with the Biacore 3000 instrument software, where the on- and off-rate constants for CsA over the particular surface were predetermined and fixed for the fitting process.

Intrinsic tryptophan fluorescence binding assays

CypA possesses a single tryptophan residue (Trp121) that is near (~9 Å) the substrate proline binding pocket of the active site. The structure of CsA bound to CypA shows a strong H-bonded interaction between Trp121 and the carbonyl oxygen of MeLeu9 in CsA [33]. In addition to this interaction contributing significantly to the binding affinity and specificity of CsA for CypA, it accounts for the spectral changes in the fluorescence of Trp121 observed on complex formation [34]. Binding of CsA produces an enhancement of approximately two- to threefold and roughly an 8-nm blue shift in the tryptophan emission maxima (from 350 to 242 nm). Fluorescence emission spectra for CypA and His-CypA were obtained on a PTI Quantmaster spectrofluorometer (Photon Technology International) in a 3-ml cuvette at 25 °C under constant gentle stirring. Tryptophan fluorescence was excited at 295 nm (5 nm bandpass), and emission was measured at 342 nm (5 nm bandpass). CypA (0.2–1 μM) was incubated in the absence or presence of increasing amounts of CsA in 25 mM Tris (pH 7.5), 100 mM NaCl, 1–2% ethanol, and 1 mM NaN_3 for 60 min at 25 °C, and the emission spectra were measured.

Steady-state binding assays

We assumed that any change in the fluorescence signal at 342 nm is proportional to the concentration of CypA:ligand complex. The observed fluorescence was buffer background subtracted and corrected for dilution and inner filter effects by Eq. (1):

$$f_{\mathrm{corr}} = \{(\mathrm{vol}_0 + \mathrm{vol}_{\mathrm{add}}/\mathrm{vol}_0) \times f_{\mathrm{obs}}\}/e^{(-2.303 \times \varepsilon_{295\mathrm{nm}} \times L \times [\mathrm{Lig}])}, \quad (1)$$

where f_{corr} is the corrected fluorescence signal, f_{obs} is the observed fluorescence signal, $\varepsilon_{295\mathrm{nm}}$ is the ligand extinction coefficient at 295 nm (CsA, 985 M^{-1} cm^{-1}), L is the path length (in this case 0.5 cm), and [Lig] is the molar ligand concentration. The corrected fluorescence signal, f_{corr} (in arbitrary units), on complex formation can be defined as

$$f_{\mathrm{corr}} = f_{\mathrm{f}} + (f_{\mathrm{b}} - f_{\mathrm{f}}), \quad (2)$$

where f_{f} is the fluorescence of free uncomplexed CypA and f_{b} is the fluorescence of the CypA:ligand complex at infinite concentration of ligand. At any total concentration of CypA [CypA], f depends on the total ligand [Lig] concentration and the dissociation equilibrium constant for the complex (K_{d}) according to Eq. (3). The data were least squares fit to Eq. (3) using Kaleidagraph v3.6 software (Synergy Software):

$$f_{\mathrm{corr}} = f_{\mathrm{f}} + (f_{\mathrm{b}} - f_{\mathrm{f}}) \times \{(K_{\mathrm{d}} + [\mathrm{CypA}] + [\mathrm{Lig}]) - \sqrt{((K_{\mathrm{d}} + [\mathrm{CypA}] + [\mathrm{Lig}])^2 - (4 \times [\mathrm{CypA}] \times [\mathrm{Lig}]))/2 \times [\mathrm{Lig}]}\}. \quad (3)$$

Determination of kinetic rate constants for CsA binding to CypA

The interaction of CsA and CypA was followed by monitoring the enhancement in the intrinsic tryptophan fluorescence of CypA (reported in arbitrary units) at 25 °C in a 3-ml cuvette under constant gentle stirring on a PTI Quantmaster spectrofluorometer, with excitation at 295 nm and emission at 342 nm (5 nm slit width for both). CypA was used at a final concentration of 0.25 μM in 25 mM Tris (pH 7.5), 100 mM NaCl, 0.5 mM DTT, 0.5 mM EDTA, and 1% ethanol. Various concentrations of CsA were added to the CypA mixture, and the solution was mixed and placed in the fluorometer with a total dead time of approximately 3 s. The on- and off-rate constants ($k_{+\mathrm{CsA}}$ and $k_{-\mathrm{CsA}}$, respectively) were determined by fitting the fluorescence enhancement at 342 nm as a function of time to reaction 1, indicated below, and least squares minimization fitting of the data using version 8.01 of the Berkeley Madonna package. CsA is the CsA concentration and CypA is the concentration of recombinant human CypA:

$$\mathrm{Reaction1}: \mathrm{CsA} + \mathrm{CypA} \leftrightarrow \mathrm{CsA}:\mathrm{CypA} \quad k_{+\mathrm{CsA}};\ k_{-\mathrm{CsA}}.$$

Competition fluorescence experiments

If a second nonfluorescent ligand, [LigB], that has negligible effect on the fluorescence intensity of CypA

itself competes with CsA, [CsA] for binding Cyp-A, [CypA], then a plot of the corrected fluorescence, f_{corr}, versus the concentration of competing ligand, in the presence of a fixed amount of [CsA], can be fitted to Eq. (4) to give the apparent K_i for the competing ligand. Such data were least squares fit to Eq. (4) using Kaleidagraph v3.6 software:

$$f_{corr} = f_f + (f_b - f_f)/\{(K_d \times (([LigB] + K_i))/K_i \times [CypA_o]) + 1\}, \quad (4)$$

where K_d is the equilibrium dissociation constant for CsA binding to CypA, [LigB] is the concentration of the competing ligand, K_i is the equilibrium dissociation constant of the competing ligand and CypA, and [$CypA_o$] is the free concentration of CypA at [LigB] = 0.

Miscellaneous

The molecular weights of CsA, CypA, and His-CypA are 1202.12, 18,012, and 20,307 Da, respectively. Protein concentration was determined by measurement of absorbance at 280 nm and was calculated using the extinction coefficient 8490 M^{-1} cm^{-1}. The molecular weights of compounds KM19, KM184, KM198, and CD291/02 are 372.5, 412.5, 430.5, and 322.5 Da, respectively.

Results

Generation of a stable NTA-His-CypA sensor surface

Between approximately 1000 and 3200 RU of pure His-CypA could be captured on an NTA sensor surface using recommended protocols (Fig. 1A). However, the affinity of the single hexahistidine tag for the Ni^{2+}–NTA moiety on the chip is relatively weak ($K_d \sim 0.5$–3 μM [12]), and immediately after the injection phase (Fig. 1A, phase a) is halted there is significant and steady baseline drift due to dissociation of the histidine tag from the chip surface (Fig. 1A, phase b). All of the initially immobilized protein could be dissociated from the surface by washing with running buffer for approximately 2 h (Fig. 1A, *). Such a sensor surface is not really stable enough for the determination of binding constants, especially for potentially weakly binding and low-molecular weight ligands.

Complete elimination of protein dissociation was achieved by rapidly following the capture of His-CypA on the NTA surface with a brief covalent stabilization phase (Fig. 1B). After saturation responses were achieved (Fig. 1B, phase a), a 30-s burst of surface activation and coupling (with a mixture of NHS/EDC, Fig. 1B, phase c) was quickly followed by a 30-s injection of ethanolamine (Fig. 1A, phase d) to quench the unreacted succinimide esters remaining on the sensor surface (see Materials and methods). The dissociation of His-CypA from the sensor surface was completely arrested. Even after washing the surface exhaustively (⩾3 h) with running buffer, the response level remained constant (Fig. 1B).

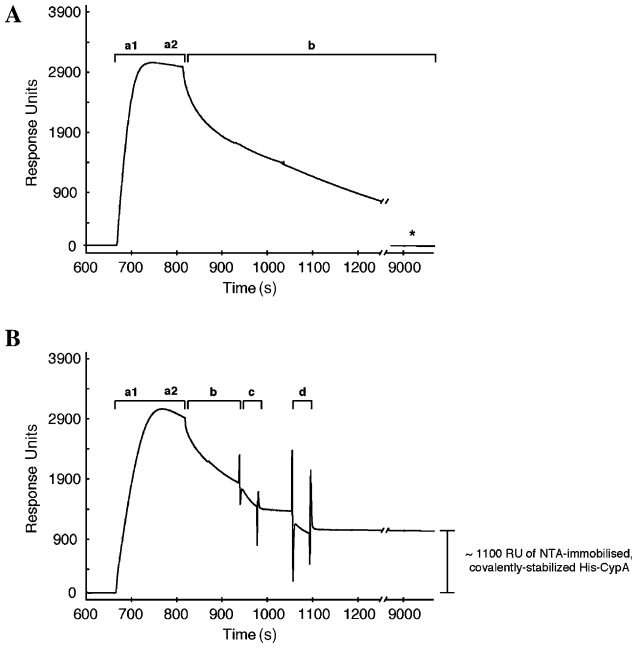

Fig. 1. Generation of a stable NTA-His-CypA sensor surface. Panels A and B show the reference-corrected sensorgrams corresponding to the injection (phases a1–a2) of 850 nM His-CypA over a Ni^{2+}–NTA sensor surface. (A) After saturation of the signal response (~3100 RU in this experiment), the injection of protein was stopped and the sensor surface was washed with 10 mM Hepes (pH 7.4), 150 mM NaCl, 0.005% surfactant P20, and 2% ethanol at 5 μl min^{-1} for 2.5 h. The response signal drops steadily due to His-CypA dissociating from the surface (phase b). Phase a2, where a slight drop in the response signal is observed during the injection phase, is likely due to a loss of rebinding [12] resulting from the relatively high concentration of His-CypA passed over the surface. For all concentrations of His-CypA tested (200 nM–1 μM), all of the initially immobilized protein could be completely dissociated form the Ni^{2+}–NTA surface after washing with running buffer for ⩾2 h (*). (B) Following saturation of the RU signal (phases a1–a2), a 30-s injection (at 15 μl min^{-1}) of a mixture of NHS (115 mg ml^{-1}) and EDC (750 mg ml^{-1}) (phase c), followed immediately by a 30-s injection (at 15 μl min^{-1}) of 1 M ethanolamine (pH 8.5) (phase d), was performed. This brief covalent stabilization phase, via primary amine coupling, eliminates the slow dissociation of the histidine tag from the NTA moiety (phase b) on the sensor surface. The final amount of His-CypA covalently immobilized on the surface was between approximately 850 and 1600 RU.

Using standard protocols, significant levels (~1000–5000 RU) of pure CypA and biotinylated CypA could also be covalently immobilized on activated CM5 and SA sensor surfaces, respectively (data not shown) [35] (see Materials and methods). These surfaces exhibited stable response levels with no baseline drift (data not shown).

Activity of NTA-captured, covalently stabilized His-CypA

Next, we wanted to assess the activity of the immobilized protein on the sensor surfaces. This was performed by passing saturating concentrations (>0.95 μM) of the naturally occurring tight binding ligand ($K_d \sim 10$–40 nM, Table 1) CsA over the sensor surfaces. CsA is a cyclic undecapeptide fungal metabolite with immunosuppressive properties that is widely used in transplant surgery [13]. The surface activity of various sensor surfaces is represented graphically in Fig. 2. His-CypA captured and covalently stabilized on the NTA surface retained very high levels of activity, typically in excess of 85% (Fig. 2A). In comparison, the immobilized protein on the surface of the CM5 chips retained only approximately 5% activity (Fig. 2B). Similarly, only 7% activity was retained by biotinylated CypA immobilized on an SA sensor surface (Fig. 2B). Pure CypA was biotinylated using standard primary amine coupling chemistries before immobilization on the SA chip (see Materials and methods).

We used the covalently stabilized His-CypA sensor surfaces to further characterize the interaction of CypA with CsA. Globally fitting a kinetic model where a 1:1 complex is formed between His-CypA and CsA to data similar to those illustrated in Fig. 3A gave very good fits. The mean on-rate constant (k_{+CsA}) was 0.53 ± 0.1 μM^{-1} s^{-1}, and the mean off-rate constant (k_{-CsA}) was 0.012 ± 0.01 s^{-1}, giving an equilibrium dissociation constant (K_{dCsA}) of 23 ± 6 nM (Table 1). The inclusion of mass transport considerations had only a very minor effect on the kinetic constants extracted from the data. Very similar values for K_{dCsA} were obtained from steady-state response calculations, where the mean K_{dCsA} value was 18.5 ± 6 nM (Fig. 3B and Table 1). These values determined by SPR for the equilibrium dissociation constant for CsA binding to His-CypA are in good agreement with those determined from solution fluorescence titration experiments ($K_{dCsA} = 29 \pm 6$ nM, Fig. 4) and with values determined by other methods in the literature (for a representative comparison, see Table 1).

Our values for the apparent kinetic rate constants, determined from SPR experiments, also agree well with those determined from modeling the time course of the CsA binding-induced fluorescence enhancement (Fig. 4B and Table 1) and with those recently published for the interaction of the CypD isoform and CsA ana-

Table 1
Representative equilibrium dissociation (K_{dCsA}), on-rate constant (k_{+CsA}), and off-rate constant (k_{-CsA}) for the interaction of CsA with CypA, His-CypA, or CypD, determined from this study and other studies

	K^{Eq}_{dCsA} (nM)	K^{Kin}_{dCsA} (nM)	k_{+CsA} (μM^{-1} s^{-1})	$k_{-CsA} \times 10^{-3}$ (s^{-1})
SPR				
His-CypA[a]	18.5 ± 6	23 ± 6	0.53 ± 0.1	12 ± 1
CypA[b]	38.5 ± 10.4	—	—	—
CypD[c]	—	12.5 ± 1	0.25 ± 0.1	3.9 ± 1
TcypD-hAGT[c]	—	12.8 ± 1	0.39 ± 0.1	4.8 ± 1
Tryptophan fluorescence				
CypA[a]	26 ± 9	16 ± 9	0.45 ± 0.13	7 ± 2
His-CypA[a]	29 ± 13	—	—	—
CypA[d]	46	—	—	—
CypD[c]	12.5 ± 4	—	—	—
ITC				
CypA[e]	11.4 ± 3.9	—	—	—
CypA[f]	47.6	—	—	—
PPIase assay				
CypA[a]	6.3 ± 3.8	—	—	—
CypA[g]	1.6 ± 0.4	—	—	—
CypA[h]	20			

Note. K^{Eq}_{dCsA} values were determined from steady-state experiments using the indicated technique. K^{Kin}_{dCsA} values were calculated from kinetic assays using the determined on-rate (k_{-CsA}) and off-rate (k_{+CsA}) constants from SPR experiments or from intrinsic tryptophan fluorescence time course experiments using the formula $K_{dCsA} = k_{-CsA}/k_{+CsA}$.

[a] Values (means ± SE, where $n \geqslant 3$) determined from this study.

[b] [39].

[c] Values determined by SPR in [32] using CsA and either human CypD or a fusion of O^6-alkylguanine-DNA-alkyltransferase and CypD (TCypD-hAGT).

[d] [43].

[e] Values determined using ITC in [36].

[f] Values determined using ITC in [44].

[g] $K_{i,app}$ values determined using a PPIase enzymatic assay performed as described in [45,46].

[h] $K_{i,app}$ values determined using a PPIase enzymatic assay performed as described in [45,47].

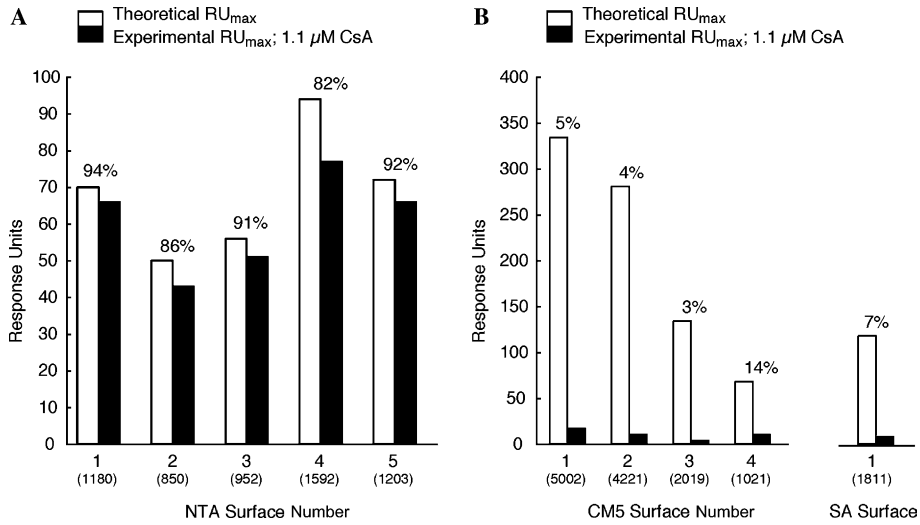

Fig. 2. Covalently stabilized His-CypA on the NTA sensor surface retaining high levels of activity. (A) Graphical representation comparing the theoretical maximum RU signal (white bars) with the experimental maximum RU signal (black bars) of five different NTA sensor surfaces generated as described (see Materials and methods). The activity of the protein coupled to the surface varied minimally between 85 and 95%; the specific activity of each surface is indicated. The number in parentheses below each sensor surface number is the total amount of protein (in RU) finally stabilized on the sensor surface. (B) A similar graphical representation comparing the theoretical maximum RU signal (white bars) with the experimental maximum RU signal (black bars) of CM5 and SA sensor surfaces generated as described. The average level of activity retained for the CM5 surface-immobilized CypA was 6.5%, and the level of activity retained for the single SA surface-immobilized CypA was 7%. These values appear to be relatively unaffected by the total amount of protein initially deposited on the sensor surface. In all cases, the experimental RU_{max} value was generated by passing 1.1 μM CsA in 10 mM Hepes (pH 7.4), 150 mM NaCl, 3 mM EDTA, 0.005% surfactant P20, and 2% ethanol over the surface.

lyzed by SPR [32]. In the study by Huber and coworkers [32], the apparent on and off rates for CsA binding to CypD ranged between 0.2 and 0.5 $\mu M^{-1}\ s^{-1}$ (on rate) and between 0.003 and 0.006 s^{-1} (off rate), giving a mean K_{dCsA} of 12 nM [32] (Table 1).

Our sensor surfaces generated by this method gave responses that were very reproducible. Three independent runs of 25 nM CsA over the same sensor surface 4 h apart gave sensorgrams that are virtually superimposable (Fig. 3C). Locally fitting each curve gave essentially identical on- and off-rate constants (data not shown). In addition to a high level of run reproducibility, the saturation responses with CsA varied minimally over the course of many hours (Fig. 3D). Essentially the same response was observed for $\geqslant$38 h.

These results indicate that the simple protocol of first capturing His-CypA on a Ni^{2+}–NTA chip and then briefly covalently stabilizing it, using standard primary amine coupling chemistries, generates a very stable and active sensor surface. They further suggest that in terms of binding affinities and kinetics, His-CypA is interacting with CsA in a manner similar to that in free solution.

Competition SPR binding assay

We have previously generated several novel combinatorial libraries of small molecule inhibitors of human CypA (K. Malone, C. Dunsmore, N.J. Turner, unpublished results). We wanted to test whether the His-CypA sensor surfaces described in the above sections could be used to facilitate the primary screening of these small-molecule (M_r ~300–500 Da) ligand libraries. Fig. 5A graphically illustrates the equilibrium response signal attained for 120 μM of the respective ligands. These compounds were chosen as positive controls to assess the sensor surface because they have previously been shown to bind to CypA with K_d values in the 10- to 100-μM range (Table 2). One problem encountered was that the ligands tested have limited solubility in aqueous buffers, and this led to significant variation in the response signals for repeat runs of the same ligand. In addition, large ''spikes'' in the RU signal at the beginning and end of the injection phases further hampered reliable direct detection (data not shown). These can likely be attributed to a bulk phase shift given that there are large amounts of insoluble material present during the mobile phase as it passes over the chip surface with protein attached. Ethanol (2%) was added to the running buffer to help ligand solubility for all runs. Higher concentrations of either ethanol or methanol resulted in protein denaturation and rapid loss of activity on the sensor surface on subsequent runs (data not shown). DMSO was avoided as a solvent because this binds to CypA itself, albeit very weakly [31]. Nevertheless, direct binding to His-CypA could be detected for the ligands KM19, KM184, KM198, and CD291/02 (Fig. 5A).

We also used a competition binding assay in which a fixed concentration of CsA (25 nM, a concentration near the K_{dCsA} value, Table 1) was passed over the

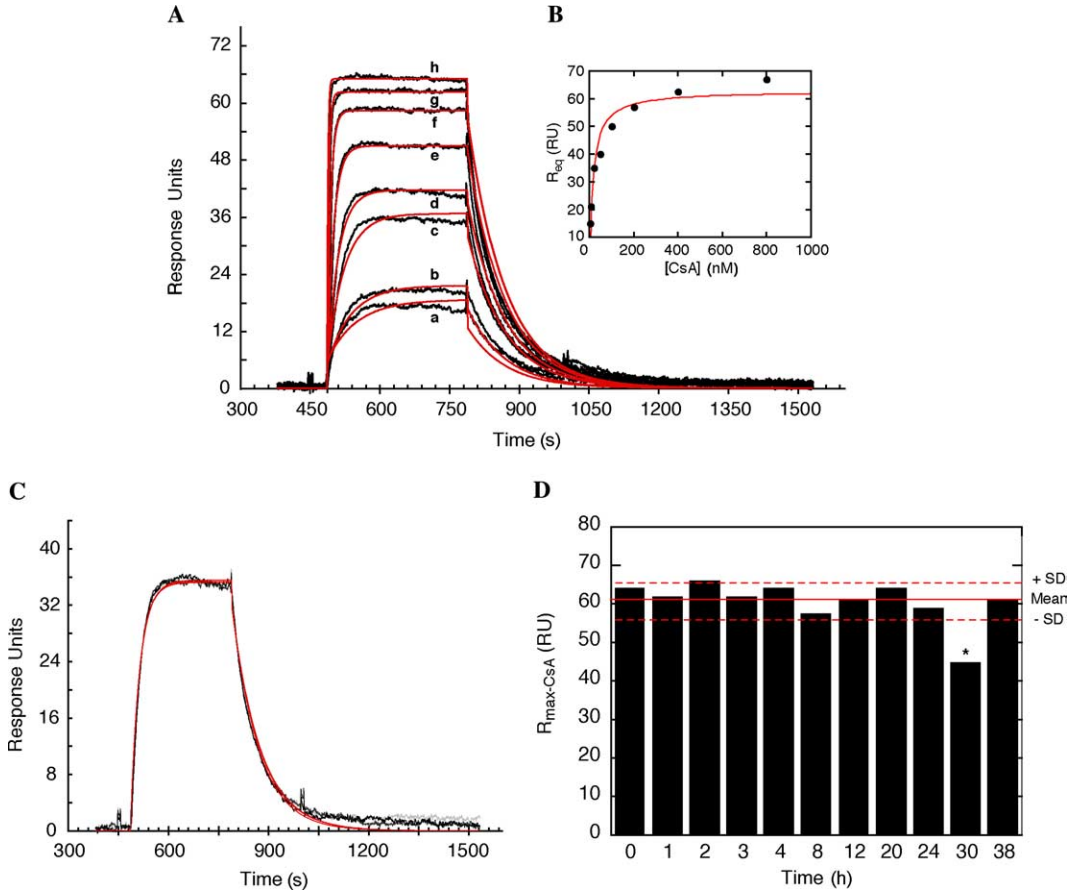

Fig. 3. Binding of CsA to covalently stabilized His-CypA. (A) Reference-corrected SPR binding curves (black) for various concentrations of CsA monitored on a surface with 1180 RU of covalently stabilized His-CypA. The data were globally fitted (red) using a kinetic model where a 1:1 complex is formed between His-CypA and CsA. From this experiment, the apparent on-rate constant (k_{+CsA}) is 0.49 μM^{-1} s^{-1} and the apparent off-rate constant (k_{-CsA}) is 0.011 s^{-1}, giving an equilibrium dissociation constant (K_{dCsA}) of 20.4 nM for CsA binding to His-CypA. Running buffer was 10 mM Hepes (pH 7.4), 150 mM NaCl, 3 mM EDTA, 0.005% surfactant P20, and 2% ethanol. Curve a, 3 nM CsA; curve b, 6 nM CsA; curve c, 20 nM CsA; curve d, 50 nM CsA; curve e, 100 nM CsA; curve f, 200 CsA; curve g, 400 nM CsA; curve h, 800 nM CsA. (B) Plot of steady-state response units, R_{eq}, versus the concentration of CsA in nanomolars gives an apparent K_d of 18 ± 3 nM. (C) Three repeat runs of 20 nM CsA over the same surface, 4 h apart, illustrate the high run reproducibility of the sensor surface. All three sensorgrams are essentially identical and lie on top of one another. Locally fitting the data (red lines) with a 1:1 complex model gave essentially identical values for the on- and off-rate constants (data not shown). (D) The covalently immobilized His-CypA surface is stable over long periods of time. The saturated response unit values ($R_{max\text{-}CsA}$) are plotted versus time in hours for individual repeat runs of 1 μM CsA over the same NTA-His-CypA sensor surface. The mean value $R_{max\text{-}CsA}$ for this particular sensor surface was 61 RU (solid red line). The theoretical RU_{max} value for this surface is 72 RU (1203 RU of His-CypA immobilized). The dashed red lines indicate ±SD (5.6 RU). Only 1 (*) of the 11 repeat runs over the course of approximately 40 h falls significantly outside ±1 SD about the mean maximum RU signal. (For interpretation of the references to color in this figure legend, the reader is referred to the web version of this article.)

sensor surface in the absence or presence of increasing concentrations of the small-molecule inhibitors. Fig. 5B illustrates a representative set of sensorgrams from such experiments. The sensorgrams obtained from such assays were generally less noisy than those obtained in direct binding experiments. Three small molecules (KM184, KM19, and KM198) were tested and competed with CsA for binding to CypA with K_d values in the micromolar range (Table 2). The rank ordering of the compounds from tightest to weakest binding was as follows: KM184, KM19, and KM198 with K_d values of 36, 46.9, and 73.6 μM, respectively (Table 2). Relatively similar K_d values, and (more important) the same rank order, were obtained for these three compounds in solution by a fluorescence competition assay (data not shown) (Table 2).

Discussion

Covalent coupling of proteins via primary amines is frequently the method of choice for immobilization in SPR assays, generating sensor surfaces with high ligand density and no baseline drift. Our results here illustrate, however, that CypA is not amenable to direct covalent linkage using primary amines. Protein activity levels

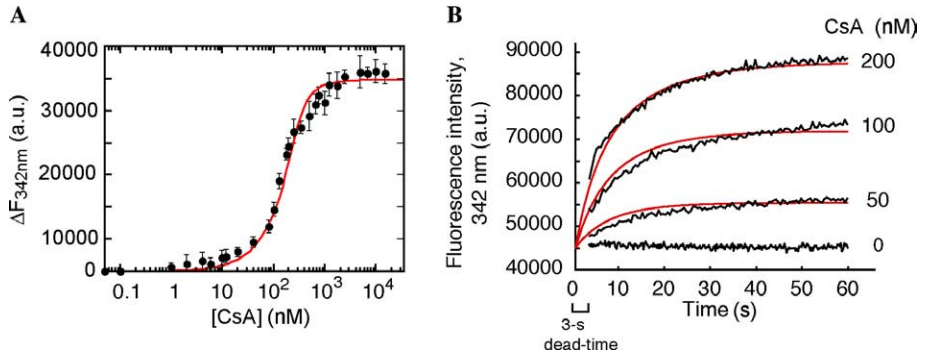

Fig. 4. Binding of CsA to CypA in solution. (A) At saturating concentrations of CsA, the intrinsic tryptophan fluorescence emission spectra of CypA shows an enhancement of approximately twofold and a blue shift of approximately 8 nm in the emission maxima, from 350 to 342 nm, compared with protein alone [34]. The steady-state fluorescence enhancement at 342 nm (ΔF_{342nm}) of 0.25 μM CypA is plotted versus the concentration of CsA in nanomolars. Each point is the mean of three separate measurements ±SE. The data were least squares fit (solid black line) to Eq. (3) (see Materials and methods), giving an apparent K_{dCSA} of 25 ± 6 nM ($n = 9$) for the binding of CsA to CypA. Essentially identical values were obtained with His-CypA (Table 1). (B) The time course of the fluorescence enhancement of 0.25 μM CypA (black lines) on the addition of various concentrations of CsA (indicated) is shown. The red lines are a least squares fit of the data to a kinetic model, as described in Materials and methods. The 3-s dead time for recording the data is indicated, whereas the fitted lines start at $t = 0$. The mean apparent on and off rates for CsA binding to CypA are 0.45 ± 0.13 μM^{-1} s^{-1} and 0.007 ± 0.002 s^{-1}, respectively, giving a K_{dCsA} of 16 ± 8.6 nM (Table 1). a.u., arbitrary units. (For interpretation of the references to color in this figure legend, the reader is referred to the web version of this article.)

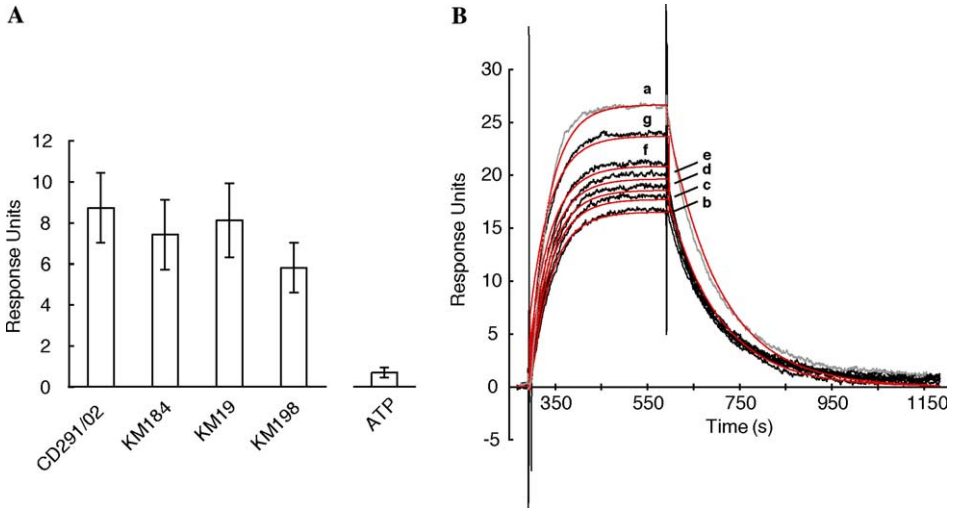

Fig. 5. Binding of small-molecule inhibitors to His-CypA. (A) Graphical representation comparing the mean (from three repeat runs, with error bars showing ±SE) equilibrium response signal for a sensor in contact with 120 μM of the respective small-molecule CypA inhibitors. ATP (120 μM), an unrelated molecule of similar molecular weight (505 Da), is shown as a control for nonspecific interactions with the surface. (B) KM19 competes with CsA for binding to His-CypA. Reference-corrected SPR binding curves (black) for various concentrations of KM19 in the presence of a fixed concentration of CsA (25 nM) were monitored on an NTA surface with 952 RU of covalently stabilized His-CypA. The data were globally fitted (red) using the competing analyte, single binding site model supplied with the Biacore 3000 machine software, where the on- and off-rate constants for CsA were calculated from a concentration series similar to that in Fig. 3A and fixed at 0.49 μM^{-1} s^{-1} and 0.01 s^{-1}, respectively (red line over gray sensorgram, $K_{dCsA} = 21$ nM). The apparent equilibrium dissociation constant (K_d) of KM19 for His-CypA is 46.9 μM, with on and off rates of 6.6×10^{-3} μM^{-1} s^{-1} and 0.031 s^{-1}, respectively. Curve a, 25 nM CsA alone; curve b, 25 nM CsA + 1.6 μM KM19; curve c, 25 nM CsA + 3.12 μM KM19; curve d, 25 nM CsA + 6.25 μM KM19; curve e, 25 nM CsA + 12 μM KM19; curve f, 25 nM CsA + 25 μM KM19; curve g, 25 nM CsA + 62.5 μM KM19. The $R_{max\text{-}CsA}$ for this particular sensor surface was 51 RU. The theoretical maximum RU value for this surface is 56 RU. (For interpretation of the references to color in this figure legend, the reader is referred to the web version of this article.)

for CypA directly immobilized on CM5 surfaces were only approximately 5%. This activity was unaffected by the initial immobilization levels; immobilization of between 1000 and 5000 RU of untagged CypA gave essentially the same low levels of activity (Fig. 2B). The X-ray structure indicates that the majority of CypA's 16 primary amines (15 lysine residues and the N terminus) are surface exposed [33] and probably available for direct covalent linkage. However, the surface electrostatic potential of CypA (Fig. 6) illustrates that the front face (the CsA binding face) is strikingly basic, whereas the rear face is much more acidic in character.

Table 2
Equilibrium dissociation and rate constants for interaction of small-molecule dimedone derivative ligands with CypA

Ligand	Molecular weight (Da)	k_+ (μM^{-1} s^{-1})	$k_{-(s^{-1})}$	K_{dBia} (μM)	K_{dFluor} (μM)
KM184	412.5	0.58×10^{-3}	0.021	36	12.2 ± 9.2 ($n = 5$)
KM19	372.5	0.66×10^{-3}	0.031	46.9	15.1 ± 8.2 ($n = 3$)
KM198	430.5	0.53×10^{-3}	0.039	73.6	29 ± 21.3 ($n = 3$)

Note. K_{dBia} values were calculated from the off- and on-rate constants (k_- and k_+, respectively) determined from SPR competition experiments in the presence of 25 nM CsA and using the formula $K_{dBia} = k_-/k_+$. Mean K_{dFluor} values were determined from competition fluorescence titration experiments (see Materials and methods) (data not shown).

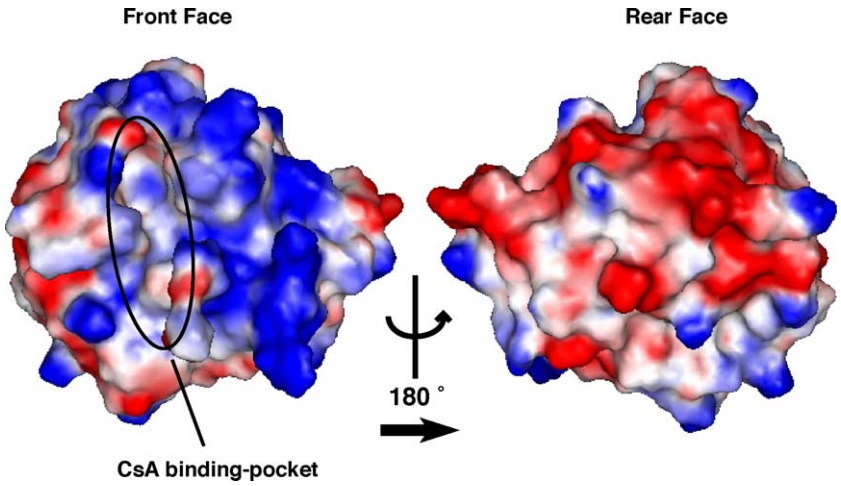

Fig. 6. Electrostatic potential surfaces for CypA. The surfaces are viewed from the front CsA binding face (left) and are rotated 180° from the rear face (right). The CsA binding pocket is indicated on the left panel. The electrostatic potential at the surface is color coded from most positive (blue) through to most negative (red).

Under the solution conditions (pH 4.9) used during the immobilization process, the surface charge potential of CypA seems likely to force the molecule to orient itself with the CsA binding surface oriented downward toward the activated chip surface. Thus, most of the covalent linkage would occur via residues on the CsA binding surface, resulting in severe steric occlusion of the binding of CsA. The activity levels of CypD immobilized by direct covalent linkage, under similar conditions and with similar final protein immobilization levels, were approximately 45 to 65% [32]. However, CypD does not possess the same markedly polarized surface charge potential of CypA; thus, coupling via primary amines is unlikely to take place predominantly on the CsA binding face.

In addition to these structural/steric considerations, the pH of 4.9 used during the initial immobilization phase likely further contributes to the low protein activity on CM5 chips. The K_{dCsA} at pH 4.9 was 150 nM ± 34 nM (determined from fluorescence titration experiments [data not shown]), compared with 26 ± 9 nM at pH 7.5 (Fig. 4 and Table 1). Similar acidic pH shift-dependent affinity loss has been observed in isothermal titration calorimetry (ITC) experiments with CypA and CsA [36], attributed to protein protonation effects. The protein recovers only partially; when the pH was raised again to 7.5, the K_{dCsA} for the same sample of CypA as above was 57 ± 12 nM (data not shown). It is unclear why protonation would not be reversible other than some partial irreversible denaturation due to the acidic solution conditions that for CypA does occur at a pH below 5 [17,36].

In contrast to these observations, the simple protocol described here for immobilizing and covalently stabilizing His-CypA yields a very stable ($\geqslant$38 h), highly active ($\geqslant$85% activity), and sensitive sensor surface. Using the N-terminal histidine tag to first capture CypA on the NTA sensor surface seems to provide a measure of orientation for the immobilized protein. The 10-amino acid linker between the hexahistidine tag and the start of the CypA sequence likely lifts CypA away from the active chip surface, preventing coupling to random lysine residues that hinder/prevent CsA binding. The only primary amine near enough to the activated sensor surface is the N terminus, and the entropic effects of being immobilized near the surface via the histidine tag may provide specificity for coupling essentially only to this primary amine. Thus, the protein is covalently immobilized but is kept active and sterically competent for CsA binding.

It is interesting to note that the apparent on-rate constants for CsA binding to either CypA or CypD

isoforms determined in this study (~0.5 μM^{-1} s^{-1}) and in that by Huber and coworkers (~0.3 μM^{-1} s^{-1}) [32] are somewhat slower than a diffusion limited on rate (~10 μM^{-1} s^{-1}), as one might have expected for a relatively small molecule such as CsA (M_r ~1200 Da). The hydrophobic cyclic undecapeptide CsA is in multistate equilibrium between two extreme conformations influenced by the solution conditions. In aqueous solution, CsA tends more to adopt a compact closed conformation [37], whereas cyclophilins bind tightly only to an open conformation. The slower than diffusion limit on-rate constants might reflect the CsA conformational equilibrium. The off-rate constant for the CypA:CsA interaction appears to be two- to threefold quicker than that between CsA and CypD (0.012 and 0.004 s^{-1}, respectively [32]) (Table 1). This slight difference may reflect genuine differences in the molecular details of the interaction between CsA and these two differentially localized, functionally distinct cyclophilin isoforms. CypA is ubiquitously localized in mammalian cytoplasm [13], whereas CypD is a mitochondrial-targeted PPIase [38]. Nevertheless, the binding constants obtained in this study for the equilibrium dissociation constant for CsA binding to His-CypA by SPR agree well with the values for the same interaction determined by a variety of experimental approaches, including ITC, intrinsic tryptophan fluorescence, and PPIase enzymatic assays (Table 1). This does suggest that the protein molecules immobilized on the chip surface behave in a manner comparable to that of protein molecules in solution, at least in terms of binding to CsA.

The results in this study illustrate the sensitivity of SPR in that we were able to reliably detect the direct binding of small-molecular weight ligands (300–500 Da) (Fig. 5A). However, the on rates for these small-molecule inhibitors are very slow (~0.4–0.7×10^{-3} μM^{-1} s^{-1}) (Table 2), orders of magnitude slower than even CsA itself. Although they appear to bind specifically to CypA, there may be some conformational constraint on these small molecules that requires a degree of "induced fit" in terms of their binding mechanism. Structural data of these cyclophilin–ligand complexes are not available, and the bound conformation of the ligands is not known. Poor solubility, aggregation, and/or nonspecific binding of the ligands may also play a role in the calculation of their apparently slow on rate, and it is possible that the functional ligand concentration, competent to interact with the immobilized His-CypA, is less than the expected measured total. This would result in the apparent on rates being faster and the equilibrium dissociation constants being tighter. However, this is unlikely to cause orders of magnitude changes in these kinetic constants. It is reassuring to note that despite the slow calculated on rates, the apparent K_d values for these ligands and the rank order of their relative affinities determined from the competition experiments agree with the values determined by intrinsic tryptophan fluorescence experiments.

This study is the first to use SPR to analyze small-molecule–CypA binding interactions. Indeed, this article also provides the first published values for the on and off rates of the CypA–CsA interaction. The protocol is simple and yields a sensor with high levels of immobilized protein activity that leads to sensors with a high degree of sensitivity. There are relatively few studies in the literature that report the use of SPR in the study of CypA and its binding partner interactions [28–30,32,39–42]. In early work analyzing the interaction of CypA and CsA and the conformational requirements required for this interaction [39–41], CsA (conjugated to bovine serum albumin [BSA]) and not CypA, was immobilized on the sensor surface [39]. Although interactions between CypA, directly coupled to the sensor surface, and protein binding partners have been published (e.g., HIV-1 capsid [28], HIV-1 Vpr [42], SARS coronavirus [30]), the activity and sensitivity of a sensor surface needed to detect binding in these much larger molecules are significantly less than those required to detect small molecules.

A further advantage of the surfaces generated in this study is that they are very unlikely to exhibit problems with steric hindrance due to the "overcrowding" of molecules on the surface, a potential problem with immobilization of relatively high amounts of protein. The average level of His-CypA finally stabilized on the NTA sensor surfaces in this study was approximately 1000 RU. This corresponds to approximately 3×10^{10} protein molecules within a volume of approximately 1×10^{14} nm^3 and provides an average intermolecular spacing between each CypA molecule of more than 100 Å This rather sparse but stable binding arrangement may explain the good agreement in the values for the kinetic and equilibrium constants among the SPR data, the solution fluorescence data, and other published data determined by other techniques.

Conclusions

The results in this study clearly indicate that CypA is not amenable to direct covalent coupling to SPR sensors via primary amines. Conversely, our study provides a good general methodology for generating a highly sensitive, stable, and reusable sensor surface of His-CypA that interacts with CsA in a manner essentially indistinguishable from that determined by other experimental approaches. Furthermore, it provides a good methodology that would allow the development of a medium-throughput screen for small molecules ligands/inhibitors of CypA that may provide useful leads in developing new drugs for the treatment of diseases such as HIV and malaria.

Acknowledgments

We thank John Butler of Biacore for invaluable technical support, advice, and an inordinate amount of patience. This work was supported by the MRC, Biacore, the Wellcome Trust, and the Edinburgh Protein Interaction Centre (EPIC).

References

[1] D.G. Myszka, Kinetic, equilibrium, and thermodynamic analysis of macromolecular interactions with Biacore, Methods Enzymol. 323 (2000) 325–340.
[2] J.M. McDonnell, Surface plasmon resonance: towards an understanding of the mechanisms of biological molecular recognition, Curr. Opin. Chem. Biol. 5 (2001) 572–577.
[3] M. Buckle, Surface plasmon resonance applied to DNA–protein complexes, Methods Mol. Biol. 148 (2001) 535–546.
[4] R.L. Rich, D.G. Myszka, A survey of the year 2002 commercial optical biosensor literature, J. Mol. Recognit. 16 (2003) 351–382.
[5] D.G. Myszka, R.L. Rich, Implementing surface plasmon resonance biosensors in drug discovery, Pharm. Sci. Technol. Today 3 (2000) 310–317.
[6] C.L. Baird, E.S. Courtenay, D.G. Myszka, Surface plasmon resonance characterization of drug/liposome interactions, Anal. Biochem. 310 (2002) 93–99.
[7] Y.N. Abdiche, D.G. Myszka, Probing the mechanism of drug/lipid membrane interactions using Biacore, Anal. Biochem. 328 (2004) 233–243.
[8] D.G. Myszka, Analysis of small-molecule interactions using Biacore S51 technology, Anal. Biochem. 329 (2004) 316–323.
[9] M.J. Cannon, G.A. Papalia, I. Navratilova, R.J. Fisher, L.R. Roberts, K.M. Worthy, et al., Comparative analyses of a small molecule/enzyme interaction by multiple users of Biacore technology, Anal. Biochem. 330 (2004) 98–113.
[10] S. Lofas, Optimizing the hit-to-lead process using SPR analysis, Assay Drug Dev. Technol. 2 (2004) 407–415.
[11] A. Zhukov, M. Schurenberg, O. Jansson, D. Areskoug, J. Buijs, Integration of surface plasmon resonance with mass spectrometry: automated ligand fishing and sample preparation for MALDI MS using a Biacore 3000 biosensor, J. Biomol. Tech. 15 (2004) 112–119.
[12] L. Nieba, S.E. Nieba-Axmann, A. Persson, M. Hamalainen, F. Edebratt, A. Hansson, et al., Biacore analysis of histidine-tagged proteins using a chelating NTA sensor chip, Anal. Biochem. 252 (1997) 217–228.
[13] A. Galat, Peptidylprolyl *cis*/*trans* isomerases (immunophilins): biological diversity–targets–functions, Curr. Top. Med. Chem. 3 (2003) 1315–1347.
[14] G.J. Towers, T. Hatziioannou, S. Cowan, S.P. Goff, J. Luban, P.D. Bieniasz, Cyclophilin A modulates the sensitivity of HIV-1 to host restriction factors, Nat. Med. 9 (2003) 1138–1143.
[15] C.S. Gavigan, S.P. Kiely, J. Hirtzlin, A. Bell, Cyclosporin-binding proteins of *Plasmodium falciparum*, Intl. J. Parasitol. 33 (2003) 987–996.
[16] J. Dornan, P. Taylor, M.D. Walkinshaw, Structures of immunophilins and their ligand complexes, Curr. Top. Med. Chem. 3 (2003) 1392–1409.
[17] R.E. Handschumacher, M.W. Harding, J. Rice, R.J. Drugge, D.W. Speicher, Cyclophilin: a specific cytosolic binding protein for cyclosporin A, Science 226 (1984) 544–547.
[18] P. Rovira, L. Mascarell, P. Truffa-Bachi, The impact of immunosuppressive drugs on the analysis of T cell activation, Curr. Med. Chem. 7 (2000) 673–692.
[19] M.K. Hu, A. Badger, D.H. Rich, Cyclosporin analogs modified in the 3,7,8-positions: substituent effects on peptidylprolyl isomerase inhibition and immunosuppressive activity are nonadditive, J. Med. Chem. 38 (1995) 4164–4170.
[20] J. Kallen, V. Mikol, P. Taylor, M.D. Walkinshaw, X-ray structures and analysis of 11 cyclosporin derivatives complexed with cyclophilin A, J. Mol. Biol. 283 (1998) 435–449.
[21] M. Evers, J.C. Barriere, G. Bashiardes, A. Bousseau, J.C. Carry, N. Dereu, et al., Synthesis of non-immunosuppressive cyclophilin-binding cyclosporin A derivatives as potential anti-HIV-1 drugs, Bioorg. Med. Chem. Lett. 13 (2003) 4415–4419.
[22] L. Wei, J.P. Steiner, G.S. Hamilton, Y.Q. Wu, Synthesis and neurotrophic activity of nonimmunosuppressant cyclosporin A derivatives, Bioorg. Med. Chem. Lett. 14 (2004) 4549–4551.
[23] R. Baumgrass, Y. Zhang, F. Erdmann, A. Thiel, M. Weiwad, A. Radbruch, G. Fischer, Substitution in position 3 of cyclosporin A abolishes the cyclophilin-mediated gain-of-function mechanism but not immunosuppression, J. Biol. Chem. 279 (2004) 2470–2479.
[24] J. Bua, A.M. Ruiz, M. Potenza, L.E. Fichera, In vitro antiparasitic activity of cyclosporin A analogs on *Trypanosoma cruzi*, Bioorg. Med. Chem. Lett. 14 (2004) 4633–4637.
[25] Y. Zhang, F. Erdmann, R. Baumgrass, M. Schutkowski, G. Fischer, Unexpected side chain effects at residue 8 of cyclosporin A derivatives allow photoswitching of immunosuppression, J. Biol. Chem. 280 (2005) 4842–4850.
[26] A. Pahl, M. Zhang, K. Torok, H. Kuss, U. Friedrich, Z. Magyar, et al., Anti-inflammatory effects of a cyclosporin receptor-binding compound, D-43787, J. Pharmacol. Exp. Ther. 301 (2002) 738–746.
[27] Y.Q. Wu, S. Belyakov, C. Choi, D. Limburg, I.B. Thomas, M. Vaal, et al., Synthesis and biological evaluation of non-peptidic cyclophilin ligands, J. Med. Chem. 46 (2003) 1112–1115.
[28] S. Yoo, D.G. Myszka, C. Yeh, M. McMurray, C.P. Hill, W.I. Sundquist, Molecular recognition in the HIV-1 capsid/cyclophilin A complex, J. Mol. Biol. 269 (1997) 780–795.
[29] T. Horibe, C. Yosho, S. Okada, M. Tsukamoto, H. Nagai, Y. Hagiwara, et al., The chaperone activity of protein disulfide isomerase is affected by cyclophilin B and cyclosporin A in vitro, J. Biochem. (Tokyo) 132 (2002) 401–407.
[30] C. Luo, H. Luo, S. Zheng, C. Gui, L. Yue, C. Yu, et al., Nucleocapsid protein of SARS coronavirus tightly binds to human cyclophilin A, Biochem. Biophys. Res. Commun. 321 (2004) 557–565.
[31] G. Kontopidis, P. Taylor, M.D. Walkinshaw, Enzymatic and structural characterization of non-peptide ligand–cyclophilin complexes, Acta Crystallogr. D Biol. Crystallogr. 60 (2004) 479–485.
[32] W. Huber, S. Perspicace, J. Kohler, F. Muller, D. Schlatter, SPR-based interaction studies with small molecular weight ligands using hAGT fusion proteins, Anal. Biochem. 333 (2004) 280–288.
[33] J. Kallen, C. Spitzfaden, M.G. Zurini, G. Wider, H. Widmer, K. Wuthrich, M.D. Walkinshaw, Structure of human cyclophilin and its binding site for cyclosporin A determined by X-ray crystallography and NMR spectroscopy, Nature 353 (1991) 276–279.
[34] M. Gastmans, G. Volckaert, Y. Engelborghs, Tryptophan microstate reshuffling upon the binding of cyclosporin A to human cyclophilin A, Proteins 35 (1999) 464–474.
[35] B. Johnsson, S. Lofas, G. Lindquist, Immobilization of proteins to a carboxymethyldextran-modified gold surface for biospecific interaction analysis in surface plasmon resonance sensors, Anal. Biochem. 198 (1991) 268–277.
[36] J. Fanghänel, G. Fischer, Thermodynamic characterization of the interaction of human cyclophilin 18 with cyclosporin A, Biophys. Chem. 100 (2003) 351–366.
[37] D. Altschuh, W. Braun, J. Kallen, V. Mikol, C. Spitzfaden, J. Thierry, Conformational polymorphism of cyclosporin A, Structure 2 (1994) 963–972.

[38] K.Y. Woodfield, N.T. Price, A.P. Halestrap, cDNA cloning of rat mitochondrial cyclophilin, Biochim. Biophys. Acta 1351 (1997) 27–30.
[39] G. Zeder-Lutz, R. Wenger, M.H. Van Regenmortel, D. Altschuh, Interaction of cyclosporin A with an Fab fragment or cyclophilin: affinity measurements and time-dependent changes in binding, FEBS Lett. 326 (1993) 153–157.
[40] G. Zeder-Lutz, M.H. Van Regenmortel, R. Wenger, D. Altschuh, Interaction of cyclosporin A and two cyclosporin analogs with cyclophilin: relationship between structure and binding, J. Chromatogr. B Biomed. Appl. 662 (1994) 301–306.
[41] G. Zeder-Lutz, N. Rauffer, D. Altschuh, M.H. Van Regenmortel, Analysis of cyclosporin interactions with antibodies and cyclophilin using the BIAcore, J. Immunol. Methods 183 (1995) 131–140.
[42] K. Zander, M.P. Sherman, U. Tessmer, K. Bruns, V. Wray, A.T. Prechtel, et al., Cyclophilin A interacts with HIV-1 Vpr and is required for its functional expression, J. Biol. Chem. 278 (2003) 43202–43213.
[43] J. Liu, C.T. Walsh, Peptidyl-prolyl *cis-trans*-isomerase from *Escherichia coli*: a periplasmic homolog of cyclophilin that is not inhibited by cyclosporin A, Proc. Natl. Acad. Sci. USA 87 (1990) 4028–4032.
[44] D. Seebach, H.G. Bossler, R. Flowers, E.M. Arnett, Calorimetric measurements of the complexation of cyclosporine A, ascomycin, fujimycin, and rapamycin with lithium-chloride and with an immunophilin, Helv. Chim. Acta 77 (1994) 291–305.
[45] J.L. Kofron, P. Kuzmic, V. Kishore, E. Colon-Bonilla, D.H. Rich, Determination of kinetic constants for peptidyl prolyl *cis-trans* isomerases by an improved spectrophotometric assay, Biochemistry 30 (1991) 6127–6134.
[46] M.J. Bossard, P.L. Koser, M. Brandt, D.J. Bergsma, M.A. Levy, A single Trp121 to Ala121 mutation in human cyclophilin alters cyclosporin A affinity and peptidyl-prolyl isomerase activity, Biochem. Biophys. Res. Commun. 176 (1991) 1142–1148.
[47] J.L. Kofron, P. Kuzmic, V. Kishore, G. Gemmecker, S.W. Fesik, D.H. Rich, Lithium chloride perturbation of *cis-trans* peptide bond equilibria: effect on conformational equilibria in cyclosporin-A and on time-dependent inhibition of cyclophilin, J. Am. Chem. Soc. 114 (1992) 2670–2675.